

# Modulating *Miox2* expression in *nicotiana tabacum* and impacts on genes involved in cell wall biosynthesis

NASCIMENTO, Daniela Defavari do

CONTI, Gabriela

LABATE, Mônica T. V.

GUTMANIS, Gunta

BERTOLLO, Ana L. F.

ANDRADE, Alexander de

BRAGATTO, Juliano

PAGOTTO, Luís Otávio

DAMIN, Plínio

MOON, David H.

LABATE, Carlos A. \*

\* Corresponding author - *E-mail address*: [calabate@usp.br](mailto:calabate@usp.br)

## Abstract

Cell walls are essential structures for plant development and growth. Apart from its biological functions, the polysaccharides that make cell walls (cellulose, hemicellulose and pectins) are the principal natural fibrous materials, considered the most important renewable resource on earth, used as raw material for many industrial processes among them, for pulp and paper production, charcoal, and biofuels. For all these reasons, the study of molecular composition and biosynthesis of plant cell walls has been a matter of great interest for researchers over the past few years. In this context, a full-length cDNA fragment of *Miox2* gene was cloned from *Arabidopsis* seedlings, using RT-PCR, with an open reading frame of 954 pb and a corresponding protein subunit molecular mass of 37 kDa. The deduced amino acid sequence of the cDNA showed a high degree of identity with *myo*-Inositol oxygenases from other organisms. This cDNA was used for genetic transformation of tobacco, a model plant, which expressed either antisense or sense RNA. Transgenic homozygous tobacco plants, with either repression or constitutively expression of *Miox2*, were obtained with the number of copies varying from 1 to 7. Neither, the repression of the endogenous tobacco *Miox* genes or the constitutive expression of *Miox2* gene, caused major impacts on plant development, leaf morphology or flowering time. Moreover, although statistically significant ( $P < 0.05$ ) changes in the arabinan and D-galacturonate contents were observed between transgenic and control lines, these results indicate that the modulation of the *myo*-Inositol pathway caused no major impacts also on cell wall polysaccharide biosynthesis.

**Keywords:** *myo*-Inositol oxygenase; *myo*-Inositol; D-glucuronate; hemicellulose

## Resumo

As paredes celulares vegetais são estruturas essenciais para o crescimento e desenvolvimento das plantas. Além de suas diversas funções biológicas, os componentes polissacarídicos constituintes das paredes celulares (celulose, hemiceluloses e pectinas) são de vital importância como fonte natural de fibras, sendo consideradas as fontes principais de recursos renováveis do planeta, utilizados como matéria prima para diversos processos industriais, dentre eles, a produção de papel e celulose, carvão vegetal e biocombustíveis. Todos esses fatores têm despertado grande interesse no estudo da composição e biossíntese das paredes celulares. Neste contexto, um fragmento de cDNA do gene *Miox2* foi clonado de plântulas de *Arabidopsis*, via RT-PCR, com uma região aberta de leitura de 954 pb e sua proteína com massa molecular de 37kDa. A sequência deduzida de aminoácidos do cDNA apresentou alto grau de identidade com *mio*-Inositol oxigenases de outros organismos. Este cDNA foi usado para transformação genética de plantas modelo (tabaco) que produziram RNA antisense ou sense. Plantas de tabaco homozigotas para o transgene com repressão ou expressão constitutiva do gene *Miox2* foram obtidas com um número de cópias do transgene, variando de 1 a 7. A repressão do gene *Miox* de tabaco endógeno assim como a expressão constitutiva do gene *Miox2* de *Arabidopsis* não causaram alterações no desenvolvimento, morfologia foliar ou tempo de florescimento das plantas. Entretanto, alterações estatisticamente significativas ( $P < 0.05$ ) ocorreram no conteúdo de arabinana e de D-galacturonato. Estes resultados indicam que a modulação do metabolismo do *mio*-Inositol não causou grandes impactos na biossíntese dos polissacarídeos da parede celular.

**Palavras-chave:** *mio*-inositol oxigenase; *mio*-inositol; D-glucuronato; hemicelulose

## Resumen

Las paredes celulares de plantas son estructuras esenciales para el crecimiento y desarrollo de las plantas. Además de sus diferentes funciones biológicas, los polisacáridos que constituyen las paredes celulares (celulosa, hemicelulosa y pectina) son de vital importancia como fuente natural de fibra. Son asimismo considerados una de las principales fuentes de recursos renovables en el planeta y se utilizan como materia prima para muchos procesos industriales entre ellos, la producción de pulpa y papel, carbón y biocarburantes. Todos estos factores han suscitado un gran interés en el estudio de la composición y la biosíntesis de las paredes celulares. En este contexto, un fragmento de ADNc del gen *Miox2* de plántulas de *Arabidopsis* fue clonado por RT-PCR. El gen posee un marco abierto de lectura de 954 pb y codifica para una proteína cuya masa molecular es de 37kDa. La secuencia de aminoácidos deducida del ADNc evidenció un alto grado de identidad con *mio*-Inositol oxigenasas presentes en otros organismos. Este ADNc fue utilizado para la transformación genética de plantas modelo (tabaco) a través de inserciones en sentido y en antisentido. Se obtuvieron plantas de tabaco homocigotas para ambos transgenes en números de copia desde 1 a 7. La sobreexpresión y la represión del gen *Miox2* fueron corroborados adicionalmente. La represión del gen *Miox* endógeno de tabaco, así como la expresión constitutiva del gen *Miox2* de *Arabidopsis* no provocó alteraciones en el desarrollo, en la morfología foliar y en el tiempo de floración. Sin embargo, se detectaron cambios estadísticamente significativas ( $P < 0,05$ ) en el contenido de arabinano y D galacturonato. Estos resultados permitieron evidenciar un estricto control en el metabolismo de *mio*-inositol en plantas de tabaco, por lo tanto la sobreexpresión y la represión de *Miox2* fueron moduladas y no produjeron efectos importantes en la biosíntesis de polisacáridos de pared celular.

**Palabras-clave:** *myo*-inositol oxigenasa, *myo*-inositol, D-glucuronato, hemicelulosa.

**bioenergia em revista: diálogos, v. 2, n. 1, p. 60-84, jan./jun. 2012.**

NASCIMENTO, Daniela Defavari do; CONTI, Gabriela Conti; LABATE, Mônica T. V.; GUTMANIS, Gunta; BERTOLLO, Ana L. F.; ANDRADE, Alexander de; BRAGATTO, Juliano PAGOTTO, Luís Otávio; DAMIN, Plínio; MOON, David H.; LABATE, Carlos A.

*Modulating Miox2 expression in nicotiana tabacum and impacts on genes involved in cell wall biosynthesis*

---

## 1 INTRODUCTION

*myo*-Inositol is a widely distributed cyclitol found in mammalian tissues, higher plants, fungi and some bacteria, and is involved in the regulation of many metabolic processes, including signal transduction, carbohydrate metabolism, auxin biosynthesis, stress related responses, mineral nutrition, membrane biogenesis and cell wall formation (Loewus & Loewus, 1983; Majerus, 1992; Loewus & Murth, 2000; Valpuesta & Botella, 2004). Overexpression of a *Miox4* gene in *Arabidopsis thaliana* was reported as leading to an increase in the biosynthesis of ascorbic acid (Lorence et al., 2004). However, another group, working with the same transformant lines found no differences in ascorbic acid concentrations between wild type and *Miox4* overexpressing lines, concluding that *Miox* controls the metabolite level of *myo*-inositol in plants (Endres & Tenhaken, 2009). Figure 1 illustrates the pathway of *myo*-Inositol oxidation in plants and its role as an alternate route for UDP-D-glucuronate formation and the biosynthesis of uronic acids and pentoses (Feingold & Avigad, 1980; Loewus & Loewus, 1983; Loewus & Murth, 2000). Another enzyme controlling the synthesis of UDP sugars is UDP-D-glucose dehydrogenase (Dalessandro & Northcote, 1977).

In *Arabidopsis*, *myo*-inositol oxygenase is coded by a small gene family containing four members (Kanter et al., 2005). *Miox1* and *Miox2* are expressed in almost all plant tissues, whereas *Miox4* and *Miox5* are mainly expressed in flowers (Kanter et al., 2005). In order to investigate the role of the *myo*-Inositol pathway in the regulation of UDP-D-glucuronate formation, and the changes in primary cell wall composition, we cloned the *myo*-Inositol oxygenase gene (*Miox2*) from *Arabidopsis* and produced transgenic tobacco plants with either reduced expression (antisense) or constitutively expression using the CaMV 35S promoter. The impact of modulating the expression of *Miox2* in tobacco was investigated upon other genes involved in cell wall biosynthesis, such as lignin, sugar nucleotides, and cellulose.

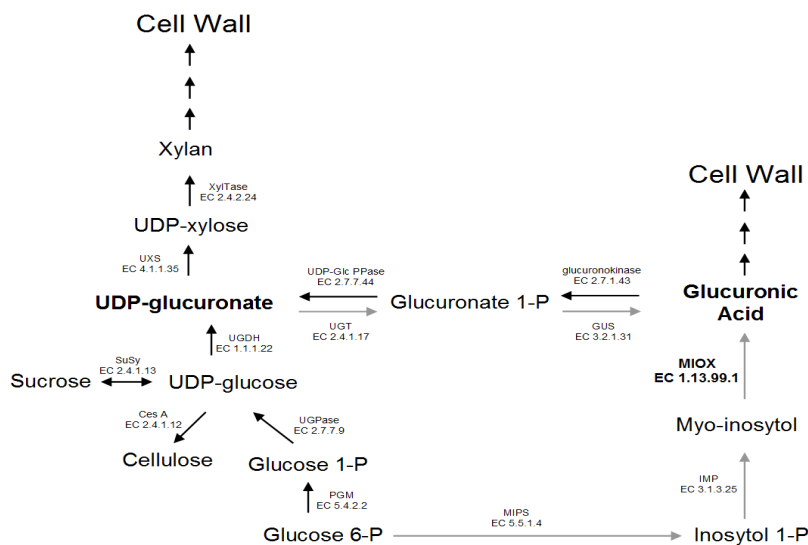


Figure 1 - *Myo*-Inositol oxidation pathway in plants and its role as an alternate route for UDP-D-glucuronate formation and the biosynthesis of uronic acids and pentoses.

## 2 MATERIAL AND METHODS

### Plant material and growth conditions

Tobacco plants (*Nicotiana tabacum* cv. Petit Havana SR1), both transgenic and wild type (WT), were grown in growth chambers under controlled conditions: 500  $\mu\text{mol m}^{-2} \text{s}^{-1}$  irradiance using a 16/8 h light/dark photoperiod and a 24°C day/18°C night temperature regime. Plants were grown in compost-vermiculite (50/50) and watered daily with a complete nutrient solution containing 10 mM nitrate and 2 mM ammonium (Hoagland & Arnon, 1950).

### Cloning and sequence analysis of the Arabidopsis *Miox2* cDNA

The sequence of the *A. thaliana Miox* from chromosome II (*Miox2*) (NM\_127538), was used to design specific primers flanking the ORF. The directional sequence CACC was added to the sense primer (MX2Forward-5'-**CACCATGACTATTCTTGTTGAACA** -3'; MX2Reverse-5'-TCACCATTTTAGTTTCGC-3') to facilitate the cloning orientation of the cDNA. Total RNA was extracted from Arabidopsis seedlings (Salzman et al., 1999). The mRNA was further purified from 75  $\mu\text{g}$  of total RNA using the Dynabeads mRNA purification kit (Invitrogen) following the manufacturer's instructions, and eluted in 20  $\mu\text{L}$  Tris-HCl 10 mM. cDNA synthesis was prepared in a 50  $\mu\text{L}$  RT-PCR (Super Script one step RT-PCR, Invitrogen) following the manufacturer's instructions. After cDNA synthesis, amplification was performed using 38 cycles of 15 s at 94°C, 30 s at 55°C, 1 min and 30 s at 72°C, followed by 7 min at 72°C. The 974-bp RT-PCR blunt-end product was cloned into the pENTR Directional TOPO Cloning vector for entry into the Gateway System available from Invitrogen. Recombinant clones, selected on kanamycin (50  $\mu\text{g mL}^{-1}$ ) were purified and screened by PCR for the presence of full-length *Miox* cDNA using *Arabidopsis Miox2* primers and by sequencing in both directions, with M13 primers, using an ABI PRISM 3100 genetic analyser (Applied Biosystems) to ensure the proper reading frame.

### Expression of the recombinant MIOX2 protein

The RT-PCR product, corresponding to the coding region of *Arabidopsis Miox2* cDNA was sub-cloned into the pDEST<sup>TM</sup>17 vector, in frame with a N-terminal 6xHis tag, for expression of the recombinant protein in *E. coli* using Gateway technology (Invitrogen). The pDEST<sup>TM</sup>17: *Miox2* construct was introduced into *E. coli* BL21-AI<sup>TM</sup> (Invitrogen). A recombinant clone, previously screened by PCR for the presence of pDEST<sup>TM</sup>17: *Miox2* insert, was grown in LB containing ampicillin (100  $\mu\text{g mL}^{-1}$ ) medium at 37°C and 200 rpm. This starter culture (1 mL, OD<sub>600nm</sub> = 0.7) was used to inoculate 50 mL of LB medium supplemented with ampicillin (100  $\mu\text{g mL}^{-1}$ ) and left to grow at 37°C (200 rpm.) until an OD<sub>600nm</sub> of 0.4 was reached. The culture was induced with 0.2% L-arabinose for 3 h, and the cells recovered by centrifugation at 13,000g for 1 min at 4°C. The pellet was ground in a mortar with 5 mL of lyses buffer

(100 mM NaH<sub>2</sub>PO<sub>4</sub>; 10 mM Tris-HCl, pH=8.0 containing 1 mM PMSF, 0.1% (w/v) lysozyme, 0.066% (v/v) β-mercaptoetanol, 0.001% (w/v) RNase and 500 U Dnase), transferred to a tube and sonicated briefly. The resulting lysate was separated into soluble and insoluble fractions by centrifugation. The fusion protein was purified from soluble fraction, using a purification column prepared with ProBond™ Nickel-Chelating Resin (Invitrogen), accordingly to the manufacturer's instructions. The purity and M<sub>r</sub> of the proteins in the eluted fractions were analysed by 10% (w/v) SDS-PAGE. The protein concentration was determined by comparing with known amounts of a standard (lysozyme) in 10% (w/v) SDS-PAGE.

### **In-gel protein digestion**

Protein spots were excised from SDS-PAGE gels, cut into small pieces (millimeters) and washed with water for 15 min. Gel pieces were washed several times with a 50% (v/v) solution containing acetonitrile (ACN) and 50 mM ammonium bicarbonate, until complete removal of the Coomassie (G250), dehydrated with 100% ACN for 10 min and rehydrated with 50 mM ammonium bicarbonate plus 20 mM dithiothreitol (DTT). After incubating for 40 min at 60°C, the supernatant was discarded and replaced by 50 mM ammonium bicarbonate with 55 mM iodoacetamide. The tubes were kept in the dark for 30 min. The gel pieces were dehydrated again with 100% ACN and let to air-dry, until complete solvent removal. The protein digestion was carried out with a solution of 10 ng μL<sup>-1</sup> trypsin (Promega), in 25 mM ammonium bicarbonate. The gel pieces were rehydrated with trypsin solution and the tubes were incubated for 12 h at 37°C. After digestion, the gel plugs were extracted twice with 50 μL of 60% (v/v) ACN, 1% (v/v) formic acid (FA) and once with 50 μL of ACN. All supernatants were combined and vacuum dried. Peptides were then suspended in 12 μL of 1% (v/v) FA for MS analysis.

### **Protein identification and analysis by LC-MS/MS**

Peptide mixtures were identified by on-line chromatography using a Cap-LC coupled to a Q-TOF Ultima API mass spectrometer (Waters, UK). Five microlitres of sample were loaded onto a NanoEase trapping column 0.18 x 23.5 mm (Waters, UK) for pre-concentration, followed by peptide separation in a LC NanoEase column Symmetry 300 C18 3.5 μm, 75 x 100 mm (Waters). Peptides were eluted in a 60 min linear gradient of solvent B [95 % (v/v) ACN, 0.1% (v/v) formic acid in water] at a flow rate of 250 nL min<sup>-1</sup>. Solvent A consisted of 5 % (v/v) ACN, 0.1% (v/v) formic acid in water. All analysis were performed using a positive ion mode at a 3 kV needle voltage. The mass range was set from 300 to 2000 m/z, and the MS/MS spectra acquired for the most intense peaks (≥ 15 counts). Multiply charged precursor ions were selected for fragmentation and peptide sequencing using automated data dependent acquisition (DDA) MassLynx software (Waters), switching from the MS to MS/MS mode and then returning to the MS. The resulting fragmented spectra were processed using the ProteinLynx v 4.0 software (Waters) and the MASCOT MS/MS Ion Search ([www.matrixscience.com](http://www.matrixscience.com)) was used to

blast the sequences against the SwissProt and NCBI databank. Combined MS-MS/MS searches were conducted with parent ion mass tolerance at 50 ppm, MS/MS mass tolerance of 0.1 Da, carbamidomethylation of cysteine (fixed modification) and methionine oxidation (variable modification). According to MASCOT probability analysis only significant ( $P < 0.05$ ) hits were accepted.

### Western blot analysis

The purified MIOX was electrophoresed on a 10% (w/v) SDS-PAGE and transferred to a PVDF membrane. The membrane was immersed in a blocking solution (TBS-T (0.05% Tween-20; 0.1 M Tris; 0.15 M NaCl, pH=7.5) containing 5% (w/v) skim milk powder) for 60 min at 37°C. This was followed by incubation with rabbit serum raised against mouse MIOX (MMIOX), kindly provided by Arner, R.J. (The Pennsylvania State University) (1:20,000), at 37°C for 60 min. The blot was washed three times in TBS-T before incubation with Anti-rabbit Ig. Horshradish - peroxidase linked whole antibody from donkey (Amersham Biosciences) (1:5,000) at 37°C for 60 min. The blot was washed three times in TBS-T and developed with the enhanced chemiluminescence detection by ECL+plus - Western blotting detection system (Amersham Biosciences), accordingly to the manufacturer's instructions. The hybridization signal was recorded on X-ray film (MXG/Plus, Kodak), between intensifying screens for 3 h, at room temperature.

### Construction of the transgenic vectors and genetic transformation of tobacco plants

The cloned RT-PCR product, corresponding to the coding region for the *Arabidopsis Miox2* cDNA was also sub-cloned into the binary Gateway Vectors (pK7WG2D and pK2WG7, Karimi et al., 2002), by recombination reaction, mediated by the LR clonase enzyme (Invitrogen) and used to transform *N. tabacum* (Horsch et al., 1985). For the repression of the *Miox2*, the directional sequence CACC was added to the reverse primer to facilitate the antisense sub-cloning of the cDNA on pK7WG2D Gateway vector (AMX2Forward 5'-ATGACTATTCITTGTTGAACA-3'; AMX2Reverse 5'-CACCTCACCATTTTAgTTTCGC-3').

The disarmed *Agrobacterium tumefaciens* strain EHA105 (Hood et al., 1986) was transformed with each recombinant Gateway binary vector (pK7WG2D/antisense-*Miox* and pK2WG7/*Miox*), by electroporation (Lilley, 1993). Recombinant clones, for each construction, selected on spectinomycin (100 µg mL<sup>-1</sup>) were purified and screened by PCR for the presence of full-length *Miox* cDNA using the *Miox2* primers. Genuine clones were grown in liquid AB medium (Ishida et al., 1996) containing spectinomycin (100 µg mL<sup>-1</sup>) at 28°C, with constant agitation (200 rpm), until OD<sub>600nm</sub> of 0.7 was reached, and used to transform *N. tabacum* cv. Petite Havana. Tobacco leaf discs were infected with each recombinant *A. tumefaciens* strain (Horsch et al., 1985), and transferred to MS medium (Murashige & Skoog, 1962) containing NAA (0.1 µg mL<sup>-1</sup>), BAP (1 µg mL<sup>-1</sup>), cefotaxime (500 µg mL<sup>-1</sup>) and kanamycin (50 µg mL<sup>-1</sup>) for shoot regeneration. Transgenic plants were selected by kanamycin resistance and verified by PCR using primers for the kanamycin resistance gene *nptII* (*nptII*Forward 5'-GCTTGGGTGGAGAGGCTATT-3'; *nptII*Reverse 5'-GCGATACCGTAAAGCAGAG-3').



Primary transformant lines showing a 700 bp amplification PCR product, corresponding to the *npII* gene were self-fertilized and the T1 seeds analysed for segregation on kanamycin using the  $X^2$  significance test. Transgenic lines showing Mendelian segregation (Budar et al., 1986) for the *npII* gene with significance ( $P < 0.05$ ) were kept for the selection of homozygous T2 progeny for further analysis.

### Southern blot analysis

Genomic DNA from homozygous T2 plants were isolated (Doyle & Doyle, 1987) and digested with *EcoRI* or *HindIII* at 37°C for 16 h. The DNA fragments were separated into a 1% (w/v) agarose gel, transferred to a Hybond-N<sup>+</sup> nylon membrane (Amersham Biosciences) by alkaline transfer (Southern, 1975; Sambrook et al., 1989). A region of the *npII* gene was labeled with Gene Images<sup>™</sup> Random Prime Labelling Module (Amersham Biosciences)

accordingly to the manufacturer's instructions. The hybridization was carried out at 55°C for 16 h, followed by stringent washes: (1 x SSC, 1% [w/v] SDS and 0.5 x SSC, 1% [w/v] SDS) at 55°C. The hybridization signal was recorded on X-ray film (MXG/Plus, Kodak), between intensifying screens for 30 min, at room temperature.

### Semi-quantitative real-time RT-PCR

Stem tissue samples collected after 3 h of illumination, from four-month-old plants, were used for total RNA isolation (Salzman et al., 1999). Poly(A) mRNA was purified from 50 µg of total RNA using the Dynabeads mRNA Purification kit (Invitrogen) as specified by the manufacturer, and eluted in 20 µL 10 mM Tris-HCl. First-strand cDNA was then generated using the SuperScript<sup>™</sup>III First-Strand Synthesis SuperMix, accordingly to the manufacturer's instructions (Invitrogen) in a 20 µL reaction mixture containing, 3/10 of the eluted mRNA and random hexamers. Semi-quantitative real-time PCR assay was performed using 1/10 of the cDNA preparation per PCR, based on preliminary cDNA quantification. Primer sequences and amplicon sizes: *Miox2 Arabidopsis* (396-bp; primers to the cloned *Arabidopsis* cDNA AtMx2Forward 5'-GAAAGTGATAGAGGAGAGGGATAA-3', AtMx2Reverse 5'-AGTGAGATGGAGCCAATCTT-3') (Kanter et al., 2005); *Miox* tobacco (156-bp, AF154639), NtMxForward 5'-GGGAAAATCCAAGACACCAA-3', NtMxReverse 5'-GCAGCATAAGGAAGAGGAGGT-3'); *ubiquitin* (203-bp, primers to the *N. tabacum* constitutive *ubiquitin* gene, UbqForward 5'-AGACATTGACTGGGAAGACC-3', UbqReverse 5'-GAGACGGAGGACAAGGTGAC-3').

To analyze the impact of the reduction or the overexpression of *myo*-Inositol oxygenase on the transcription level of other genes involved in cellulose, hemicellulose and lignin biosynthesis, we used primers for the endogenous genes involved in those metabolisms such as: CCoAOMT (295bp): *N. tabacum* caffeoyl-CoA O-methyltransferase (Z56282) NtCCoAOMT Forward 5'-GCAGCACAGGAAAATCAGGT-3', NtCCoAOMT Reverse 5'-CATCAGGAAGAGCAAGAGCA-3'; CAD1 (209bp): *N. tabacum* cinnamyl alcohol dehydrogenase 1 (AY911854) NtCAD1 Forward 5'-GCTGAAACATACCCAAATGCT-3', NtCAD1 Reverse 5'-GGAAATGGCTTATCATCAACAC-3';

4CL (297bp): *N. tabacum* 4-coumarate:coenzyme A ligase (NTU50845) Nt4CL Forward 5'-TGCTCTCTTCCTCGTAACCAA-3', Nt4CL Reverse 5'-TCCTGCCTTGCTCATCTTTCA-3'; SuSy (198bp): *N. tabacum* sucrose synthase (EU148354 and AB055497) NtSusy Forward 5'-GCTGCTGTTTAGCGATGTTG-3', NtSusy Reverse 5'-TTGGATTCCTTCCTTCGGTCT-3'; Ces (183bp): *N. tabacum* cellulose synthase (EB432590, DV161918, DV161313 and EB682114) NtCes Forward 5'-AAGGTTGAAGTGGCTGGAGA-3', NtCes Reverse 5'-GCGAAAATGGAAAGAAAGAGG-3'; Uxs1 (221bp): *N. tabacum* UDP-glucuronate decarboxylase 1 (AY619950) NtUxs1 Forward 5'-GGATTCCTGGTGACTGGTGGT-3', NtUxs1 Reverse 5'-AGGGCAAGCAAGGTGATAAA-3'; Uxs2 (229bp) *N. tabacum* UDP-glucuronate decarboxylase 2 (AY619951) NtUxs2 Forward 5'-GATGTTTGACTACCACCGACAA-3', NtUxs2 Reverse 5'-GTTTTCCCTTCATTAGCC-3'; Uxs3 (183bp) *N. tabacum* UDP-glucuronate decarboxylase 3 (AY619952) NtUxs3 Forward 5'-TTCAGACCCAACACAGCAGA-3', NtUxs3 Reverse 5'-TACGGGGAGGAGACAGAGG-3'; Uxs4 (297bp) *N. tabacum* UDP-glucuronate decarboxylase 4 (AY619953) NtUxs4 Forward 5'-TTGGCATTCTCATTGGTTCA-3' NtUxs4 Reverse 5'-TCACATTTCTTTCCTCCCAGT-3' and Ugdh (212bp) *N. tabacum* UDP-glucose dehydrogenase (AY619949 and AY619948) NtUgdh Forward 5'-AAGACCGCATCCTCACCA-3' NtUgdh Reverse 5'-AGAGCCACCAAAACCAACAC-3'.

Amplification specificity was checked by melting-curve analysis, and PCR efficiency was determined using standard curves for each primer pair constructed with serial dilutions (1:2, 1:10 and 1:100) of the cDNA preparation (Pfaffl, 2001; Pfaffl et al., 2002).

### **Extraction of cell-wall polysaccharides and lignin**

Stems of control and transgenic mature plants were harvested 3 months-post-germination in triplicate. The samples were cut into 20 cm long pieces from the basal part of the stem. The bark was removed and the remaining xylem was separated from the pith. The individualized tissues were cut into smaller pieces and frozen in liquid nitrogen. After lyophilized, the dried samples were ground in a micro-Willey cutting mill and the fine powder separated using a sieve shaker (60 mesh). Chemical removal of extractives was conducted by washing the samples in a Soxhlet extractor using toluene/ethanol (1:1) for 4 h followed by ethanol (95%) for a further 4 h period. Part of the sample (50 mg DW), free of extractives was then submitted to a strong acid hydrolysis in 500 µL of sulfuric acid (24 N) for 1 h at 30°C, followed by a mild hydrolysis, adjusting the sulfuric acid concentration to 0.86 N by adding 14 mL of water (milliQ), and autoclaving (121°C and 1 Kgf cm<sup>-2</sup>) for 1 h. The samples were cooled in an ice bath. The carbohydrates and uronic acids were determined in the soluble filtrate (after adjusting to 1 L), by pulsed amperometry, accordingly to Fardim & Duran (2001), using the ED50 Electrochemical Detector from HPLC Dionex® (ICS-2500) and CarboPac columns. Soluble lignin was determined in the filtrate spectrophotometrically at 215 and 280 nm, and the insoluble lignin by weighing the dried powder left after carbohydrate hydrolysis (TAPPI, 1991).

## Data analysis

Data collected from carbohydrate and lignin determinations were subjected to analysis of variance (ANOVA) using GLM of the SAS package. Means were compared for significance using the Dunnett's test

## 3 RESULTS AND DISCUSSION

### Cloning and characterization of the cDNA encoding Miox2 from Arabidopsis

The amino acid alignment between *Arabidopsis* MIOX2 (O82200), its isoforms MIOX1 (Q8L799), MIOX4 (Q8H1S0) and MIOX5 (Q9FJU4), *Oryza sativa* MIOX (Q5Z8T3), *Eucalyptus grandis* MIOX (ACF04280), *Solanum lycopersicum* MIOX (ACS45396) and *Sus scrofa* MIOX (NP\_999267) showed a high level of conservation among plant orthologs (Figure 2). Comparing the deduced amino acid sequences, a conserved domain DUF706 was found for all proteins, with unknown function. Primers were designed for the first 20 nucleotides from the 3' end (reverse primer) and 5' region (forward primer), adding the CACC sequence to facilitate the cloning orientation into the *Gateway* directional TOPO cloning system from Invitrogen.

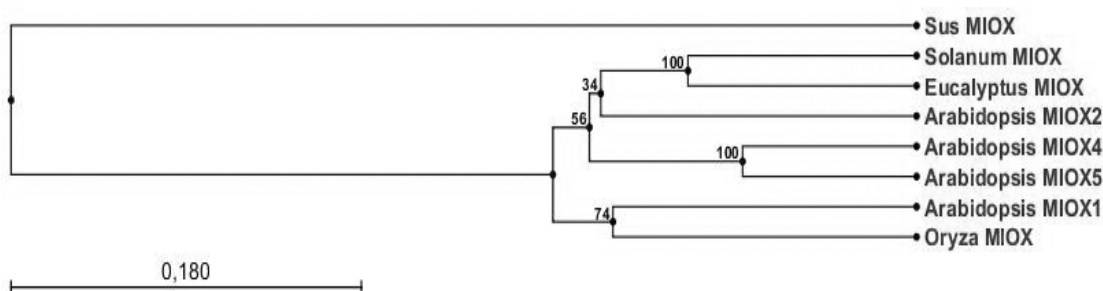


Figure 2 – The phylogenetic tree generated using CLC Main Work Bench 5.5 (UPGMA algorithm with Bootstrap analysis 100 replicates). The species and *gi* numbers are: *Arabidopsis thaliana* MIOX1, 75154124; *A. thaliana* MIOX2 75100552; *A. thaliana* MIOX4, 75151963; *A. thaliana* MIOX5, 75171102; *Oryza sativa*, 75112464; *Eucalyptus grandis*, 192338750; *Solanum lycopersicum*, 240248438; *Sus scrofa*, 47523014.

ClustalW alignment of proteins showed that the N-terminal region is not conserved (data not shown). The *Arabidopsis* MIOX2 sequence has two cysteine residues conserved at positions 179 and 215 and a total of 15 histidine residues, 7 of which are common to that reported for the *Sus scrofa* MIOX sequence (Arner et al., 2001), and other hypothetical sequences from rat, mouse and human (Yang et al., 2000; Arner et al., 2001). The presence of conserved histidine and cysteine residues in the hypothetical *Arabidopsis* amino acid sequence would indicate a role for these residues in the regulation of enzyme function, as observed in other Fe-sulphur-cluster-containing proteins (Arner et al., 2001).

### Expression of recombinant *A. thaliana* MIOX2

The polyhistidine recombinant *A. thaliana* MIOX2 protein was produced in BL21-AI™ cells (Invitrogen) and purified from the soluble fraction. The protein purification was prepared at 4°C, with a recovery of 2.5 ng  $\mu\text{L}^{-1}$ , and immediately used for enzyme assay. The recombinant protein expressed in *E. coli* catalyzed the conversion of *Myo*-inositol to glucuronic acid, confirming that the cloned cDNA encodes the MIOX enzyme (data not shown).

The Coomassie stained SDS-PAGE gel illustrates the L-arabinose induction of the MIOX2 recombinant protein in *E. coli* (Figure 3A). The protein corresponds to a monomer. The subunit molecular weight based on the translated amino acid sequence for the MIOX2 cDNA was calculated to be 37 kDa. This was further checked by electro spray mass spectrometry and SDS-PAGE. Results from mass spectrometry indicated the molecular mass to be approximately 37 kDa. SDS-PAGE indicated that the recombinant protein coded by *Miox2* has a similar molecular mass around 40KDa, as shown in Figure 3A. The slightly higher molecular mass of the recombinant MIOX2 protein is due to the presence of the 6x histidine tag with a molecular weight of 2.6KDa. Our results are in agreement with values already reported for other *Miox* gene from *A. thaliana*; the *Miox 4* located on chromosome 4, with an estimated molecular mass of 37 kDa (Lorence et al., 2004). Western immunoblot analysis using the monoclonal mouse MIOX antibodies confirmed the identity of expressed MIOX (Figure 3B).

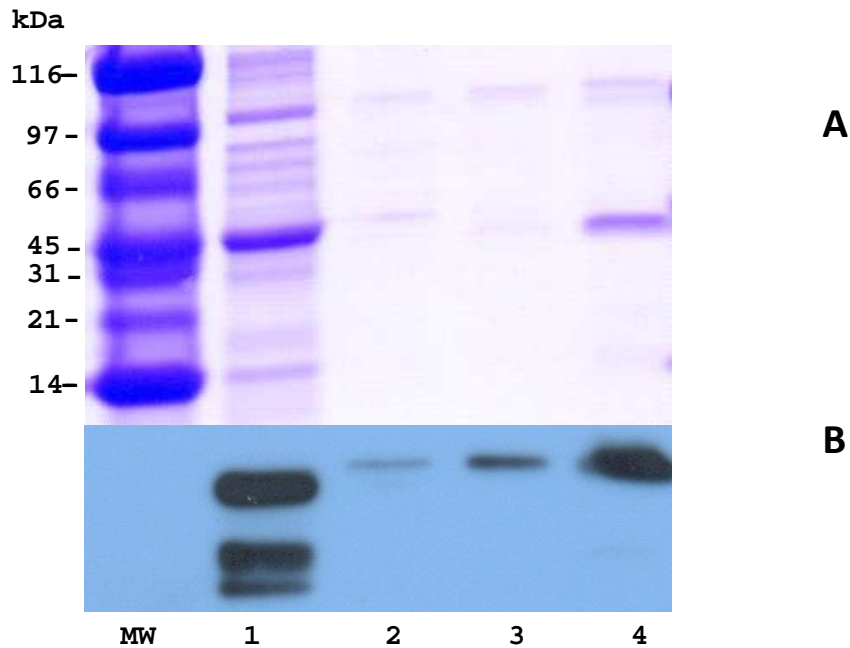


Figure 3 - (A) Coomassie stained SDS-PAGE of recombinant *Arabidopsis* MIOX2 protein. The *Miox2 A. thaliana* cDNA cloned into His-tagged pDEST expression vector was used to transform the BL21 *E. coli* cells. (B) Western blot of recombinant MIOX2 against mouse MIOX. Extracts from L-arabinose induced cells before purification (Lane 1), during wash steps (Lanes 2 and 3) and after purification (Lane 4) with a Ni column. MW, Mid-Range Protein Markers (Promega).

Table 1 - Peptides identified by mass spectrometry (<sup>a</sup> Daltons; <sup>b</sup> isoelectric point)

Name	Score	Probability	Peptide	Coverage	Mw	pI <sup>b</sup>
		%	Matches	%	Da <sup>a</sup>	
EC: 1.13.99.1	12.197	100	7	19.243	37024	5.52
Submitted Mass		Charge	Experimenta l Mass	Peptide Sequence		
751.06	3	2250.157	(R)DYPDEDWLHLTALIHVLGK(V)			
546.676	3	1637.005	(K)KNGTTLPHAGLFIIR(Y)			
504.304	3	1509.889	(K)NGTTLPHAGLFIIR(Y)			
397.876	3	1190.605	(R)IHHFYPLHK(A)			
397.884	3	1190.629	(R)YKSRYPLHK(A)			
707.424	3	2119.249	(K)VLVDVEQVKPYYISLINK(Y)			
707.399	3	2119.174	(K)VLVDVEQVKPYYISLKVK(Y)			

### Protein Sequencing

The 7 peptide sequences of *A. thaliana* MIOX2 protein isolated from L-arabinose induced BL21 *E. coli* cells, covered 19.2% of the total protein (Table 1), with an estimated molecular weight of 37.02 kDa (pI 5.52), and a probability of 100% to be the peptides (Table 1) related to the expected protein, Myo-inositol oxygenase (EC 1.13.99.1), accordingly to the blast analysis (Altschul et al., 1997).

### Genetic transformation and *Miox2* expression in *N. tabacum*

Tobacco plants were transformed with either the antisense or the constitutive recombinant *Arabidopsis Miox2* constructs. Thirty-one antisense (Anti) and thirty constitutively expressing (sense) primary transformant lines, were obtained and self-fertilized. Five T2 transformant lines of each, antisense and sense, were confirmed to be homozygous and further characterized at the molecular level. Figure 4 shows the Southern blot analysis of the transgenic lines probed with the *npII* gene. The number of transgene copies per line varied from 1 in Anti-3, 3 in Anti-2, 4 in Anti-1, 5 in Anti-4 and 7 in Anti-5 (Figure 4A). In the constitutively expressing *Miox2* plants the number of transgene copies varied from 1 in Sense-12, Sense-13 and Sense-14; 2 in Sense-10 and 3 in Sense-15 (Figure 4B). Following the quantification of the transgene copies, we analyzed the level of repression of the endogenous *Miox* gene in the stem of antisense tobacco plants (Figure 5A), and the expression of the transgene in the sense lines

(Figure 5B). Endogenous expression of tobacco *Miox* gene, in all sense lines overexpressing *A. thaliana Miox2* was not statistically different from the control line (data not shown), indicating that the overexpression of the transgene had not affected the endogenous *Miox* expression. Figure 5A shows that lines Anti-1 and Anti-5 had the highest reduction in the expression of the endogenous tobacco *Miox* gene, while line Anti-2 was not significantly repressed in relation to the control line. The transgenic lines Anti-3 and Anti-4 showed no major reduction in expression compared to control, therefore, were not kept for further analysis. The constitutively expressing *Miox2* lines (Sense-10, 12 and 14) showed a significantly higher expression than control plants (Figure 5B), while the transgenic lines Sense-13 and 15 had no major changes in transgene expression being also disconsidered in further analysis.

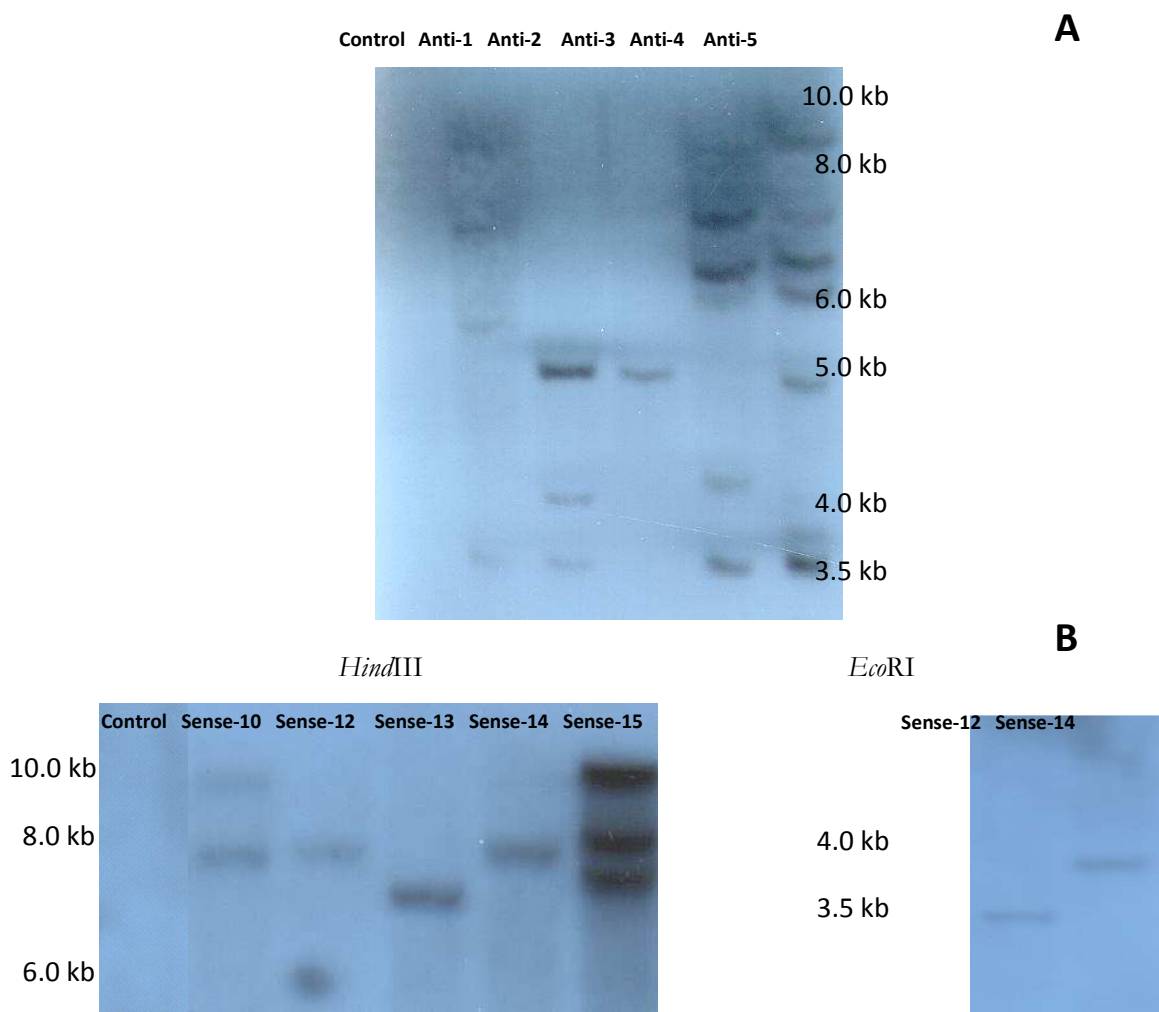


Figure 4 - (A) Genomic Southern blot of Control and transgenic anti-sense *Miox* tobacco lines (Anti 1-5), restricted with *EcoRI*; (B) Genomic Southern blot of Control and transgenic *Miox2* overexpressing tobacco lines (Sense 10-15), restricted with *HindIII* or *EcoRI*. Restriction with *EcoRI* in Sense lines 12 and 14 confirmed that they come from different transformation events. Fragment sizes are indicated in kilobase pairs (Kb).

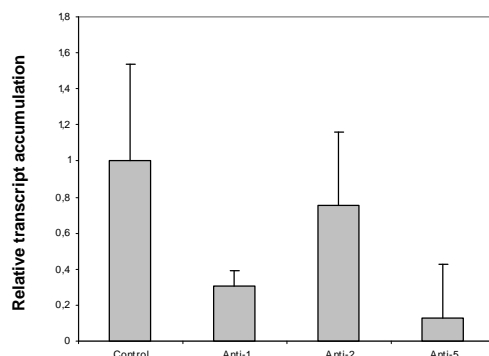
Although we were able to modulate the expression of *Miox2* in tobacco, there was no major impact on plant development, leaf morphology and flowering time (data not shown). Once no visual modifications in the transgenic plants were observed we then analyzed the expression of other genes involved in the sugar nucleotide metabolism, in both antisense and overexpressing *Miox2* plants.

### **Impact of modulation of *Miox* gene on other genes involved in cell wall polysaccharides biosynthesis**

The cell wall is composed of crystallin cellulose embedded in a hemicellulose and lignin matrix. Changes in key genes of the biosynthetic pathway, can lead to changes in the expression of other genes and/or pathways involved in cell wall polysaccharides biosynthesis. Repression of lignin biosynthesis by antisense expression of 4-coumarate coenzyme A ligase (4CL) in aspen trees was compensated by an increase in cellulose (Hu et al., 1999). Moreover, the down-regulation of O-methyltransferase (OMT) also suppressed lignin biosynthesis and increased cellulose deposition in tree species (Rastogi & Dwivedi, 2006). In the case of RNAi-mediated suppression of p-coumaroyl-CoA<sup>3'</sup>-hydroxylase (C3'H) in hybrid poplar caused altered deposition of lignin and an increase in hemicellulose and cellulose contents of woody material (Coleman et al., 2008). All those findings indicate that lignin, cellulose and hemicellulose deposition in trees may be regulated in a compensatory way that is not reported in herbaceous plants (Hu et al., 1999). Recently, the treatment of seedlings of *A. thaliana* with the phytotoxin thaxtomin A was used to inhibit cellulose synthesis. As a result, the reduction in cellulose synthesis caused ectopic lignification (Bischoff et al., 2009). To investigate possible misregulation of other genes influenced by *Miox* modulation, on cell wall biosynthesis, semi-quantitative real-time PCR was used to measure the transcript accumulation of endogenous genes involved in lignin biosynthesis, such as caffeoyl-CoA O-methyltransferase (CCoAOMT), cinnamyl alcohol dehydrogenase 1 (CAD1) and 4-coumarate coenzyme A ligase (4CL); cellulose biosynthesis, such as sucrose synthase (SuSy) and cellulose synthase (Ces) and hemicellulose biosynthesis, such as UDP-glucuronate decarboxylase (Uxs1, Uxs2, Uxs3 and Uxs4) and UDP-glucose dehydrogenase (Ugdh).



**A**



**B**

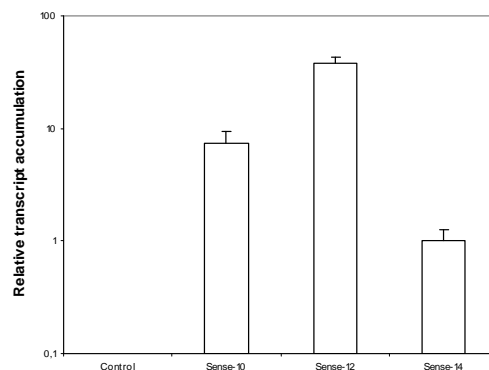


Figure 5 - (A) Semi-quantitative RT-PCR analysis of tobacco *Miox* transcript accumulation in stems of transgenic anti-sense *Miox* tobacco lines (Anti 1, 2 and 5) relative to the control, whose expression level has been assigned the value=1; (B) Semi-quantitative RT-PCR analysis of *A. thaliana Miox2* transcript accumulation in stems of transgenic *Miox2* overexpressing tobacco lines (Sense 10 and 12) relative to the Sense-14, whose expression level has been assigned the value=1. Transcript levels were normalized relative to the ubiquitin expression level used as internal standard. Results are expressed as mean of 3 replica with respective standard deviation.

The antisense transgenic line Anti-1 displayed a significant decrease in the expression of several genes analysed (Figure 6A), such as CCoAOMT, CAD1 and 4Cl (lignin pathway genes); SuSy and Ces (cellulose) and Ugdh, Uxs1 and Uxs2 (hemicelluloses). In Anti-2 line, we observed an increase in expression of Ugdh gene and of the Uxs isoforms 2, 3 and 4, possibly indicating that the reduction in the pathway of *myo*-inositol oxidation was compensated by increasing the flow and synthesis of hemicelluloses via Ugdh. In this line, there was also a trend of increased expression of cellulose synthase and sucrose synthase and a decrease in the expression of genes related to lignin metabolism as CCoAOMT and 4Cl.

Both, Sense-10 and Sense-14, transgenic lines presented an increase in Uxs isoforms and Ugdh transcripts (Figure 6B), indicating that both pathways had increased the flux and that the *myo*-inositol pathway must be of less importance for hemicelluloses and uronic acid synthesis. Lignin transcripts also had an increase in all transgenics sense lines. The Sense-12 line showed the higher increase in lignin transcripts, which could be due to the site of insertion of the transgene.

### Chemical composition of the cell wall

Uronic acids are incorporated into cell wall polysaccharides of higher plants preferentially as D-galacturonate in pectins and D-glucuronate in arabinans and xylans (Reiter & Vanzin, 2001). The formation of D-glucuronate in plants is still poorly understood. UDP-D-glucose seems to be the starting point of a series of nucleotide sugar interconversion reactions, catalyzed by UDP-D-glucose dehydrogenase, irreversibly forming UDP-glucuronate (Figure 1). However, the alternative pathway for the oxidation of *myo*-Inositol seems to play an important role in D-glucuronate formation, depending on the stage of plant development, type of tissue and growth conditions (Feingold & Avigad, 1980; Loewus & Loewus, 1983; Loewus & Murth, 2000; Seitz et al., 2000). The impact of the repression or constitutive expression of *myo*-Inositol oxygenase transcription on the composition of polysaccharides and lignin was determined in the xylem (secondary cell wall) and pith (primary cell wall) of control and transgenic tobacco lines repressed or over expressing *Miox2* (Table 2).

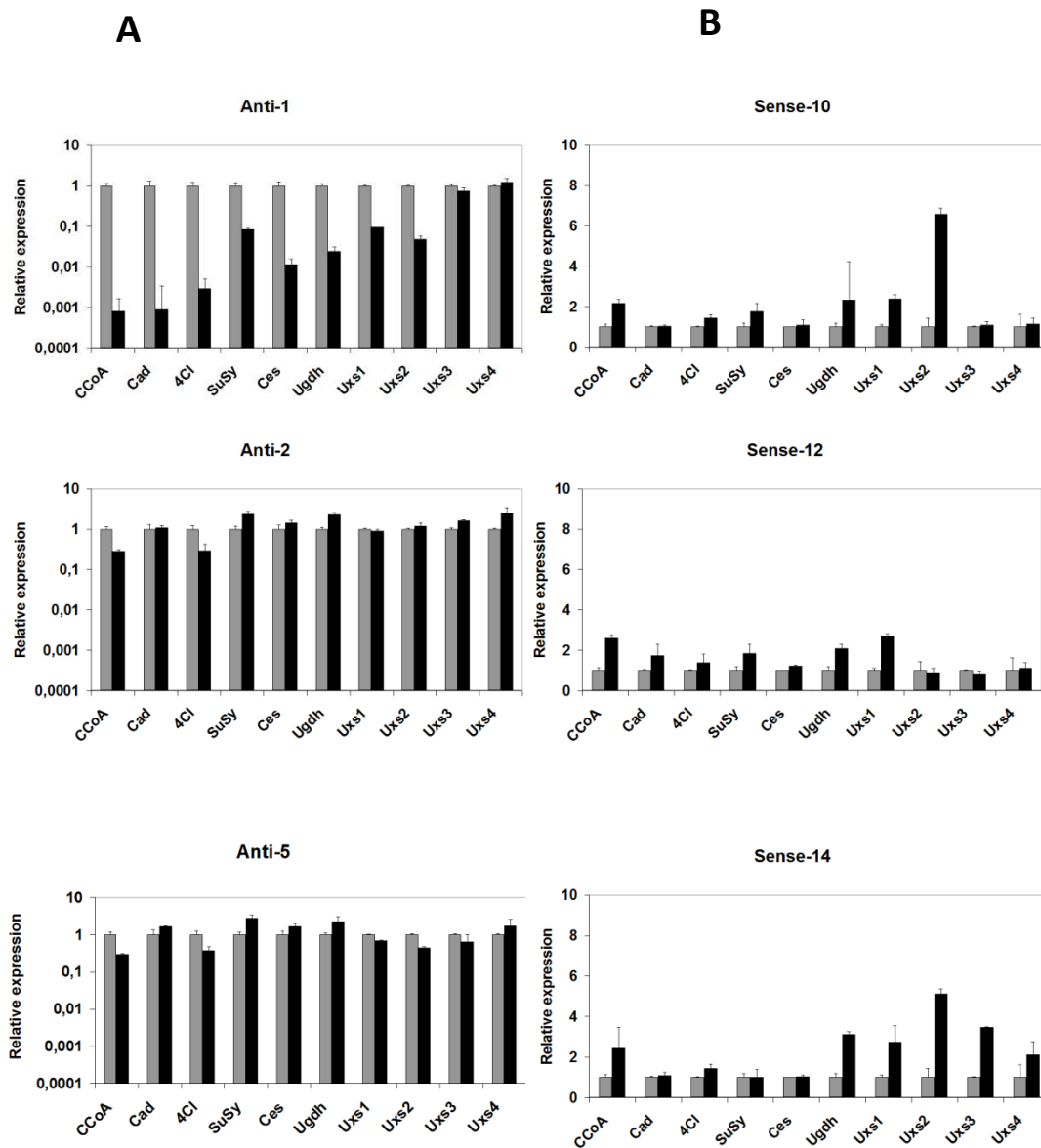


Figure 6 – Semi-quantitative RT-PCR analysis of transcripts accumulation in stems of transgenic tobacco plants by antisense (A) or over expression (B) of *A. thaliana Miox2*. Transcript levels were normalized relative to the ubiquitin expression level used as internal standard. Results are expressed as mean of 3 replica with respective standard deviation, relative to the control, which expression levels have been assigned the value=1.

There was a statistically significant ( $P < 0.05$ ) decrease in galactose and an increase in xylose at primary cell wall from pith stem (Table 2A), particularly in the anti-sense transgenic line Anti-3. As a result of the xylose increase, we observed a proportional increase of total pentoses, and consequently, of the pentose/hexose ratio, which is an important indicator of changes in the chemical composition of the cell wall. Similar results were obtained with the down-regulation of UDP-glucuronate decarboxylase in tobacco (Bindschedler et al., 2007). Plants showed high glucose to xylose ratios in xylem walls due to less xylose, while arabinose and uronic acids contents were unchanged.

The anti-sense transgenic line Anti-5 had a significant ( $P < 0.05$ ) increase of mannose and galacturonic acid at xylem (Table 2A), although the pentose/hexose ratio did not change. These results clearly indicate that the modulation of the *myo*-Inositol pathway was compensated by the UDP-D-glucose pathway (Figure 6A), causing no major impact on cell wall polysaccharide biosynthesis. Experiments of suspension-cultured *Arabidopsis* cells with [ $1\text{-}^3\text{H}$ ] D-galactose and [ $\text{U-}^{14}\text{C}$ ] D-fructose, conducted to evaluate the relative contribution of known pathways, also showed that UDP-glucose oxidation pathway predominates over *myo*-inositol oxidation (Sharples & Fry, 2007), which might be important only in early stages of development, during germination of seeds or pollen (Kärkönen, 2005) and during syncytia development induced by *Heterodera schachtii* in *Arabidopsis* roots (Siddique et al., 2009).

The primary cell wall from the pith stem of the Sense-10 *Miox2* transgenic line had a significant increase in arabinose and glucose (Table 2B). The main source of this glucose can be either cellulose or hemicellulose, since samples were totally hydrolyzed. The increase of both monosaccharides was responsible for significant increases in pentoses and hexoses, although the ratio of pentose/hexose was not significantly changed. It is interesting to observe that, in the same transgenic line, the ratio of pentose/hexose had a significant decrease in xylem (Table 2B). Another transgenic line that presented changes in the composition of the primary cell wall monosaccharides was the Sense-14, although the reduction in rhamnose and galactose may be due to alterations in the pectin layer.

#### 4 CONCLUSIONS

The repression of the endogenous tobacco *Miox* gene or the constitutive expression of the *A. thaliana Miox2* gene caused no major impact on the plant phenotype and composition of primary and secondary cell wall polysaccharides. Although we were able to detect major changes in the pattern of expression of genes involved in cell wall biosynthesis, our data provide further evidences that *myo*-Inositol oxygenase plays no major role in regulating the formation of UDP-glucuronate. These results clearly indicate that *myo*-Inositol oxidation can be compensated by the UDP-D-glucose pathway, causing no major impact on cell wall polysaccharide biosynthesis.

#### 5 ACKNOWLEDGEMENTS

This work was supported financially by the Innovation Technology Program funded by FAPESP (01/11080-8) and Suzano Papel e Celulose. Support was also provided by CAPES and CNPq with fellowships for Daniela Defavari do Nascimento, Gabriela Conti and Gunta Gutmanis, and FAPESP with fellowships for Ana Leticia Ferreira Bertollo and Plínio Damini.

We would like to thank Dr. Siu Mui Tsai and Fabiana Cannavan from CENA/ESALQ/USP and Dr Maria Helena de Souza Goldman and Andrea Carla Quiapim from FFCLRP/USP, for DNA sequencing. We also would like to thank Livia M. Franceschini for helping with the configuration of all figures.

Table 2. Polysaccharide composition (mg g<sup>-1</sup>DW) of primary cell wall (pith) and secondary cell wall (xylem) from T<sub>3</sub> (third generation progeny) transgenic and control plants. (A) Control and transgenic anti-sense *Miox* tobacco lines (Anti-1, 2 and 5); (B) Control and transgenic tobacco lines over expressing *Miox2* (Sense-10, 12 and 14). \*\* Comparisons significant at *P*<0.05 for Dunnet test.

**A**

Tobacco	Primary cell wall							Secondary cell wall							
	Ara	Man	Gal	Xyl	Glc	Gal	Gluc	Ara	Man	Gal	Xyl	Glc	Glc/Xyl	Soluble	Insoluble
Control	10.58	7.50	19.96	17.98	326.3	64.54	2.58	4.65	15.59	6.91	207.2	517.9	2.502	22.64	201.9
Anti-1	10.00	6.40	17.97	19.43	318.6	61.88	2.72	4.81	17.38	6.96	215.9	512.1	2.374**	23.82**	200.8
Anti-2	10.37	7.08	22.20	13.61	331.1	67.10	2.51	4.59	15.38	6.90	208.5	517.7	2.486	23.10	199.6
Anti-5	10.37	8.85	20.32	23.58	346.5	63.54	2.78	5.05	18.20	7.38	215.3	514.5	2.392**	22.73	200.1

**B**

Tobacco	Primary cell wall							Secondary cell wall							
	Ara	Man	Gal	Xyl	Glc	Gal	Gluc	Ara	Man	Gal	Xyl	Glc	Glc/Xyl	Soluble	Insoluble
Control	12.67	9.40	25.63	9.56	300.4	71.44	1.65	6.56	20.37	10.09	232.4	492.0	2.11	29.99	174.6
Sense-10	15.17	9.34	28.06	12.81	324.6**	72.72	1.82	6.27	19.99	9.65	228.2	496.5	2.18**	29.03	179.5
Sense-12	13.63	9.75	24.82	10.56	307.1	70.67	1.68	6.59	20.49	9.97	232.1	491.3	2.12	30.80	174.7
Sense-14	10.45	8.89	21.02**	12.50	305.7	64.57	1.66	6.23	20.21	9.47	229.3	490.2	2.14	29.51	174.5

Ara, Man, Gal, Xyl, Glc, Gal Acid, Gluc Acid: Arabinose, Mannose, Galactose, Xylose, Glucose, Galacturonic Acid and Glucuronic Acid, respectively.

## 6 REFERENCES

- ALTSCHUL, S.F.; MADDEN, T.L.; SCHAFFER, A.; ZHANG, Z.; MILLER, W.; LIMPMAN, D.J. Gapped BLAST and PSI-BLAST: A new generation of protein database search programs. *Nucleic Acids Research*. V. 25, p.3389-3402, 1997.
- ARNER, R.J.; PRABHU, K.S.; THOMPSON, J.T.; HILDENBRANDT, G.R.; LIKEN, A.D.; REDDY, C.C. Mio-inositol oxygenase: molecular cloning and expression of a unique enzyme that oxidizes *myo*-inositol and D-chiro-inositol. *Biochemistry Journal*. V. 360, p.313-320, 2001.
- BINDSCHEDLER, L.V.; TUERCK, J.; MAUNDERS, M.; RUEL, K.; PETIT-CONIL, M.; DANOUN, S.; BOUDET, A.M.; JOSELEAU, J.P.; BOLWELL, G.P. Modification of hemicellulose content by antisense down-regulation of UDP-glucuronate decarboxylase in tobacco and its consequences for cellulose extractability. *Phytochemistry*. V. 68, p.2635-2648, 2007.
- BISCHOFF, V.; COOKSON, S.J.; WU, S.; SCHEIBLE, W.R. Thaxtomin A affects CESA-complex density, expression of cell wall genes, cell wall composition, and causes ectopic lignification in *A. thaliana* seedlings. *Journal of Experimental Botany*. V. 60, p.955-965, 2009.
- BUDAR, F.; THIA-TOONG, L.; VAN MONTAGU, M.; HERNALSTEENS, J.P. *Agrobacterium* mediated gene transfer results mainly in transgenic plants transmitting T-DNA as a single Mendelian factor. *Genetics*. V.114, p.303-313, 1986.
- COLEMAN, H.D.; PARK, J.Y.; NAIR, R.; CHAPPLE, C.; MANSFIELD, S.D. RNAi-mediated suppression of p-coumaroyl-CoA 3'-hydroxylase in hybrid poplar impacts lignin deposition and soluble secondary metabolism. *Proceedings of the National Academy of Sciences*. V.105, p.4501-4506, 2008.
- DALESSANDRO, G.; NORTHCOTE, D.H. Changes in enzymatic activities of nucleoside diphosphate sugar interconversions during differentiation of cambium to xylem in sycamore and poplar. *Biochemistry Journal*. V.162, p.267-279, 1977.
- DOYLE, J.J.T.; DOYLE, J.L. Isolation of plant DNA from fresh tissue. *Focus*. V.12, p.13-15, 1987.
- ENDRES, S.; TENHAKEN, R. *myo*-Inositol oxygenase controls the level of *myo*-inositol in Arabidopsis but does not increase ascorbic acid. *Plant Physiology*. V. 149, p.1042-1049, 2009.
- FARDIM, P.; DURÁN, N. Wood and pulp carbohydrate analysis using HPLC and electrochemical detection. *Chemistry Preprint Archive, Zurich*. V. 7, p.158-163, 2001.
- FEINGOLD, D.S.; AVIGAD, G. Sugar nucleotide transformations in plants. In: STUMPF, P.K.; CONN, E.E. (eds). *The Biochemistry of Plants: A Comprehensive Treatise*, New York: Academic Press. Vol 3, 1980, p.101-170.
- HOAGLAND, D.R.; ARNON, D.I. *The water culture method of growing plants without soil*. Berkeley-USA: University of California, 1950.

**bioenergia em revista: diálogos, v. 2, n. 1, p.60-84, jan./jun. 2012.**

NASCIMENTO, Daniela Defavari do; CONTI, Gabriela Conti; LABATE, Mônica T. V.; GUTMANIS, Gunta; BERTOLLO, Ana L. F.; ANDRADE, Alexander de; BRAGATTO, Juliano PAGOTTO, Luís Otávio; DAMIN, Plínio; MOON, David H.; LABATE, Carlos A.  
*Modulating Miox2 expression in nicotiana tabacum and impacts on genes involved in cell wall biosynthesis*

---

HOOD, E.E.; HELMER, G.L.; FRALEY, R.T.; CHILTON, M.D. The hypervirulent of *Agrobacterium tumefaciens* A281 is encoded in a region of pTiBo542 outside of T-DNA. *Journal of Bacteriology*. V. 168, p.1291-1301, 1986.

HORSCH, R.B.; FRY, J.E.; HOFFMANN, N.L.; HOLTZ, E.D.; ROGERS, S.G.; FRALEY, R.T. A simple and general method for transferring genes into plants. *Science*. V. 227, p.1229-1231, 1985.

HU, W.J.; HARDING, S.A.; LUNG, J.; POPKO, J.L.; RALPH, J.; STOKKE, D.D.; TSAI, C.J.; CHIANG, V.L. Repression of lignin biosynthesis promotes cellulose accumulation and growth in transgenic trees. *Nature Biotechnology*. V. 17, p.808-812, 1999.

ISHIDA, Y.; SAITO, H.; OHTA, S.; HIEL, Y.; KOMARI, T.; KUMASHIRO, T. High efficiency transformation of maize (*Zea mays* L.) mediated by *Agrobacterium tumefaciens*. *Nature Biotechnology*. V. 14, p.745-750, 1996.

KANTER, U.; USADEL, B.; GUERINEAU, F.; LI, Y.; PULY, M.; TENHAKEN, R. The inositol oxygenase gene family of Arabidopsis is involved in the biosynthesis of nucleotide sugar precursors for cell-wall matrix polysaccharides. *Planta*. V. 221, p.243-254, 2005.

KARIMI, M.; INZÉ, D.; DEPICKER, A. Gateway vectors for *Agrobacterium*-mediated plant transformation. *Trends in Plant Science*. V. 7, p.193-195, 2002.

KÄRKÖNEN, A. Biosynthesis of UDP-GlcA: Via UDPGDH or the *myo*-inositol oxidation pathway? *Plant Biosystems - An International Journal Dealing with all Aspects of Plant Biology*. V.139, p.46-49, 2005. DOI: 10.1080/11263500500056161.

LILLEY, G. Survey number 007. In: *Gene Pulser Electroprotocol*, BIO-RAD, 1993.

LOEWUS, F.A.; LOEWUS, M.W. *myo*-Inositol: Its biosynthesis and metabolism. *Annual Review of Plant Physiology*. V. 34, p.137-161, 1983.

LOEWUS, F.A.; MURTHY, P.P.N. *myo*-Inositol metabolism in plants. *Plant Science*. V. 150, p.1-19, 2000.

LORENCE, A.; CHEVONE, B.I.; MENDES, P.; NESSLER, C.L. *myo*-Inositol Oxygenase offers a possible entry point into plant ascorbate biosynthesis. *Plant Physiology*. V. 134, p.1200-1205, 2004.

MAJERUS, P.W. Inositol phosphate biochemistry. *Annual Review of Biochemistry*. V. 61, p.225-250, 1992.

MURASHIGE, T.; SKOOG, F.A. A revised medium for rapid growth and bioassays with tobacco culture. *Physiologia Plantarum*. V. 15, p.473-497, 1962.

PFAFFL, M.W. A new mathematical model for relative quantification in real-time RT-PCR. *Nucleic Acids Research*, v.29, p.2002-2007, 2001.

PFAFFL, M.W.; Horgan, G.W.; Dempfle, L. Relative expression software tool (REST) for group-wise comparison and statistical analysis of relative expression results in real-time PCR. *Nucleic Acids Research*. V. 30, p.1-10, 2002.

**bioenergia em revista: diálogos, v. 2, n. 1, p.60-84, jan./jun. 2012.**

NASCIMENTO, Daniela Defavari do; CONTI, Gabriela Conti; LABATE, Mônica T. V.; GUTMANIS, Gunta; BERTOLLO, Ana L. F.; ANDRADE, Alexander de; BRAGATTO, Juliano PAGOTTO, Luís Otávio; DAMIN, Plínio; MOON, David H.; LABATE, Carlos A.  
*Modulating Miox2 expression in nicotiana tabacum and impacts on genes involved in cell wall biosynthesis*

---

RASTOGI, S.; DWIVEDI, U.N. Down-Regulation of Lignin Biosynthesis in Transgenic *Leucaena leucocephala* Harboring O-Methyltransferase gene. *Biotechnology Progress*. V. 22, p.609-616, 2006.

REITER, W.D.; VANZIN, G.F. Molecular genetics of nucleotide sugar interconversion pathways in plants. *Plant Molecular Biology*. V. 47, p.95-113, 2001.

SALZMAN, R.A.; FUJITA, T.; ZHU-SALZMAN, K.; HASEGAWA, P.M.; VERSAN, R.A. An Improved RNA isolation method for plant tissues containing high levels of phenolic compounds or carbohydrates. *Plant Molecular Biology Reporter*. V. 17, p.11-17, 1999.

SAMBROOK, J.; FRITSCH, E.F.; MANIATIS, T. *Molecular cloning: a laboratory manual*. Cold Spring Harbor, NY: Cold Spring Harbor Laboratory Press, 1989. 765p.

SEITZ, B.; KLOS, C.; WURM, M.; TENHAKEN, R. Matrix polysaccharide precursors in Arabidopsis cell walls are synthesized by alternate pathways with organ-specific expression patterns. *The Plant Journal*. V. 21, p.537-546, 2000.

SHARPLES, S.C.; FRY, S.C. Radioisotope ratios discriminate between competing pathways of cell wall polysaccharide and RNA biosynthesis in living plant cells. *The Plant Journal*. V. 52, p.252-262, 2007.

SIDDIQUE, S.; ENDRES, S.; ATKINS, J.M.; SZAKASITS, D.; WIECZOREC, K. HOFMANN, J.; BLAUKOPF, C.; URWIN, P.E.; TENHAKEN, R.; GRUNDLER, F.M.W.; KREIL, D.P.; BOHLMANN, H. *Myo*-inositol oxygenase genes are involved in the development of syncytia induced by *Heterodera schachtii* in Arabidopsis roots. *New Phytologist*. V. 184, p.457-472, 2009.

SOUTHERN, E.M. Detection of specific sequences among DNA fragments separated by gel electrophoresis. *Journal of Molecular Biology*. V. 98, p.503-517, 1975.

TAPPI. *Carbohydrate composition of extractive-free wood and wood pulp by liquid chromatography*, Test Method T 249 cm-85, TAPPI Test Methods, Atlanta: Ga. Technical Association of the Pulp and Paper Industry, 1991.

VALPUESTA, V.; BOTELLA, M.A. Biosynthesis of L-ascorbic acid in plants: new pathways for an old antioxidant. *Trends in Plant Science*. V. 9, p. 573-577, 2004.

YANG, Q.; DIXIT, B.; WADA, J.; WALLNER, E.I.; SRIVASTVA, S.K.; KANWAR, Y.S. Identification of a renal-specific oxido-reductase in newborn diabetic mice. *Proceedings of the National Academy of Sciences USA*. V. 97, p. 9896-9901, 2000.



**bioenergia em revista: diálogos, v. 2, n. 1, p.60-84, jan./jun. 2012.**

NASCIMENTO, Daniela Defavari do; CONTI, Gabriela Conti; LABATE, Mônica T. V.; GUTMANIS, Gunta; BERTOLLO, Ana L. F.; ANDRADE, Alexander de; BRAGATTO, Juliano PAGOTTO, Luís Otávio; DAMIN, Plínio; MOON, David H.; LABATE, Carlos A.  
*Modulating Miox2 expression in nicotiana tabacum and impacts on genes involved in cell wall biosynthesis*

---

Daniela Defavari NASCIMENTO do é doutora em agronomia, mestre em fisiologia e bioquímica de plantas pela ESALQ –USP, professora da FATEC Piracicaba. Atua na área de biotecnologia.

Gabriela CONTI é pesquisadora da FAPESP. CNIA. INTA. AR.

Gunta GUTMANIS é doutora, especialista em transformação genética, marcadores moleculares e genética.

Plínio DAMIN é engenheiro agrônomo especialista em silvicultura urbana.

Mônica T.V. LABATE é doutora em genética, chef of the Sheffield University, trabalha no laboratório Max Feffer de genética de plantas na área de biotecnologia da madeira.

Juliano BRAGATTO.

David H. MOON é professor doutor. Pesquisador do departamento de genética da ESALQ-USP.

Luís Otávio PAGOTTO. Departamento de Engenharia Florestal Colheita e Silvicultura.

Ana BERTOLLO.

Alexandre de ANDRADE.

Carlos A. LABATE é pesquisador da USP. Email: calabate@usp.br